Tailoring Second-Harmonic Generation in Birefringent Poled Fiber via Twist

E. Y. Zhu,[1,*] **L. Qian,**[1] **L. G. Helt,**[2] **M. Liscidini,**[2] **J. E. Sipe,**[2]
C. Corbari,[3] **A. Canagasabey,**[3,4] **M. Ibsen,**[3] **P. G. Kazansky,**[3]

[1]*Dept. of Electrical and Computer Engineering, University of Toronto, 10 King's College Rd., Toronto, ON M5S 3G4, Canada*
[2]*Dept. of Physics, University of Toronto, 60 St. George St., Toronto, ON M5S 1A7, Canada*
[3]*Optoelectronics Research Centre, University of Southampton, SO17 1BJ, United Kingdom*
[4]*Currently with the Optical Communications Group, University of New South Wales, Sydney 2053, Australia*
[*]*Corresponding author: eric.zhu@utoronto.ca*

Abstract: We predict theoretically and demonstrate experimentally the ability to generate and control the strengths of various second-harmonic signals in birefringent poled fiber. This is done by simply twisting the fiber.

OCIS codes: (190.4370) Nonlinear optics, fibers; (190.4410) Nonlinear optics, parametric processes

1. Introduction

The linear properties of twisted birefringent fibers have been well-studied [1]. However, studies of the nonlinear optical properties of twisted birefringent fiber have focused mainly on self-phase and cross-phase modulation [2]. Here, we report for the first time that twisting a birefringent fiber with an artificially-induced $\chi^{(2)}$ can result in the generation of new phase-matched second-harmonic (SH) signals not observed in the untwisted fiber.

We demonstrate this in a periodically poled fiber [3] with an induced $\chi^{(2)}$, which arises from a frozen-in DC field E_x^{DC} and the Kerr nonlinearity: $\chi^{(2)}_{ijk} = 3\chi^{(3)}_{ijkx}E_x^{DC}$. The non-zero $\chi^{(2)}$ tensor elements that arise from this model have been found to be experimentally valid for our fiber: $\chi^{(2)}_{xxx} = 3\chi^{(2)}_{xyy} = 3\chi^{(2)}_{yxy} = 3\chi^{(2)}_{yyx}$.

Our poled fiber is quasi-phase-matched [4] for the second-harmonic generation (SHG) of $\lambda_{SH} \approx 775$ nm light in the LP_{01} mode. The four non-zero elements of the $\chi^{(2)}$ tensor result in the presence of three distinct SHG signals ($y+y \rightarrow x$, $x+x \rightarrow x$, $y+x \rightarrow y$) with relative nonlinear transmittances in the expected ratio of 1:9:4 for the untwisted fiber (Fig. 1a). The three peaks are spectrally-separated due to the fiber birefringence at the fundamental and SH wavelengths. We attribute this to the fiber geometry (inset of Fig. 1a). The principal axes (x, y) of the fiber are aligned with the direction of the frozen-in DC field (E_x^{DC}) as again shown in the inset of Fig. 1a.

2. Theory

When a birefringent fiber is twisted, its polarization eigenmodes (X, Y) are no longer linear (x, y) but are in general elliptically-polarized [1]:

$$\vec{X} = \hat{x} - i\left(\frac{\xi}{1+\sqrt{1+\xi^2}}\right)\hat{y}, \quad \vec{Y} = \hat{y} - i\left(\frac{\xi}{1+\sqrt{1+\xi^2}}\right)\hat{x}, \quad \xi = \frac{2\Omega(1-\frac{1}{2}g)}{\beta_y - \beta_x} \tag{1}$$

where Ω is the twist rate (measured in radians per metre), g is the elasto-optic coefficient (a unitless constant, universally 0.14-0.16 for fused silica fibers [1]), and β_x (β_y) is the propagation constant for the x- (y-) polarized light in the untwisted birefringent ($\beta_x \neq \beta_y$) fiber. Note that the expressions in (1) are un-normalized. In general, the polarization eigenmodes (1) at the fundamental (ω) and second-harmonic (2ω) are different ($\vec{X}^{(\omega)} \neq \vec{X}^{(2\omega)}$) because the fiber birefringences at the two frequencies are not equal: $\left(\beta_y^{(\omega)} - \beta_x^{(\omega)}\right) \neq \left(\beta_y^{(2\omega)} - \beta_x^{(2\omega)}\right)$. In the limit where there is no twist ($\Omega \rightarrow 0$), the eigenmodes turn back into $\hat{x}$ and $\hat{y}$.

By twisting the fiber, new second-order mixings between the eigenmodes that were not allowed in the untwisted fiber can appear. Taking $\vec{X}^{(\omega)} = \hat{x} - (\epsilon)\hat{y}$, and $\vec{X}^{(2\omega)} = \hat{x} - (\delta)\hat{y}$, we can calculate the relative strengths of all these signals (Table 1). Fig. 1b plots the nonlinear transmittances of the SHG signals as a function of the twist.

Table 1. Relative Strengths of Second-Harmonic Signals in Twisted Poled Fiber

Signal	Relative Strength
$X^{(\omega)} + X^{(\omega)} \rightarrow X^{(2\omega)}$	$\left\lvert 1 + \frac{2}{3}\delta^*\epsilon + \frac{\epsilon^2}{3}\right\rvert^2$
$Y^{(\omega)} + Y^{(\omega)} \rightarrow X^{(2\omega)}$	$\left\lvert \frac{1}{3} + (\epsilon^*)^2 - \frac{2}{3}\delta^*\epsilon^*\right\rvert^2$
$Y^{(\omega)} + X^{(\omega)} \rightarrow Y^{(2\omega)}$	$4\left\lvert \frac{1}{3} - \frac{\lvert\epsilon\rvert^2}{3} + \delta\epsilon^* - \frac{\delta\epsilon}{3}\right\rvert^2$

Signal	Relative Strength
$Y^{(\omega)} + Y^{(\omega)} \rightarrow Y^{(2\omega)}$	$\left\lvert -\frac{2}{3}\epsilon^* - \frac{\delta}{3} - \delta(\epsilon^*)^2\right\rvert^2$
$X^{(\omega)} + X^{(\omega)} \rightarrow Y^{(2\omega)}$	$\left\lvert \frac{2}{3}\epsilon - \delta - \frac{1}{3}\delta\epsilon^2\right\rvert^2$
$Y^{(\omega)} + X^{(\omega)} \rightarrow X^{(2\omega)}$	$4\left\lvert -\epsilon^* + \frac{\epsilon}{3} + \frac{\delta^*}{3} - \frac{1}{3}\delta^*\lvert\epsilon\rvert^2\right\rvert^2$

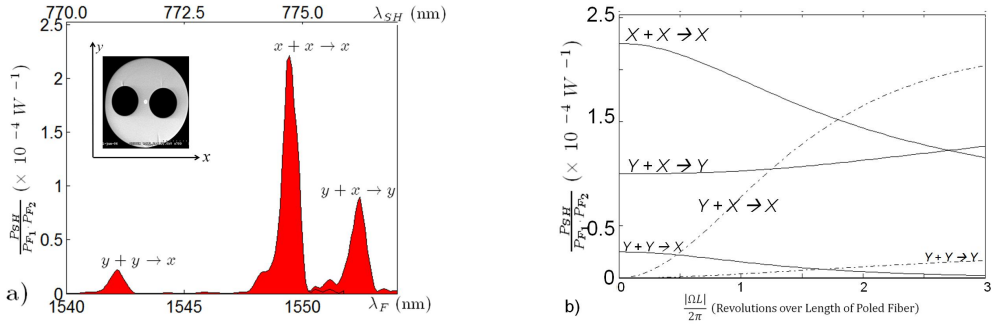

Fig. 1. a) The experimental SHG spectrum of the untwisted poled fiber, showing the expected 1:9:4 ratio of the peaks. The inset shows the fiber cross-section, where one of the principal axes (x) is also aligned to the direction of the frozen-in DC field E_x^{DC}.
b) The theoretical efficiencies of the six SHG signals listed in Table 1 are plotted as a function of twist (L is the length of the poled fiber). The efficiencies are scaled to reflect the experimentally-obtained $\chi^{(2)}$ values of the untwisted fiber. The $X + X \rightarrow Y$ signal is not labeled because its estimated efficiency is significantly smaller than the other signals.

3. Experiment

We effect a twist in the poled fiber by fixing one of its connectorized ends, while rotating the other end. A tunable CW laser source at the fundamental wavelength is used for the SHG experiment. Its polarization is adjusted with a free-space polarization controller before being launched into the poled fiber. For each value of the twist, the principal polarizations ($X^{(\omega)}$, $Y^{(\omega)}$) of the fiber are found experimentally. A wavelength sweep is performed using three polarizations ($X^{(\omega)}$, $Y^{(\omega)}$, and $X^{(\omega)} + Y^{(\omega)}$) at wavelengths where the peaks associated with the 6 SHG signals (Table 1) are expected to be. At the output of the poled fiber, the fundamental and SH beams are separated with a wavelength division multiplexer (WDM); the fundamental power and polarization are monitored with a polarimeter, while the SH power is measured with a silicon detector.

Fig. 2a plots the nonlinear transmittance of the SHG signals for various twists; they are in good agreement with the theory (the solid lines). Fig. 2b gives the experimental SHG spectrum for three values of twisting, which is also in good agreement with the theory (Fig. 2c). The theoretical nonlinear transmittances are calculated using the experimentally determined $\chi^{(2)}$ values of the untwisted fiber.

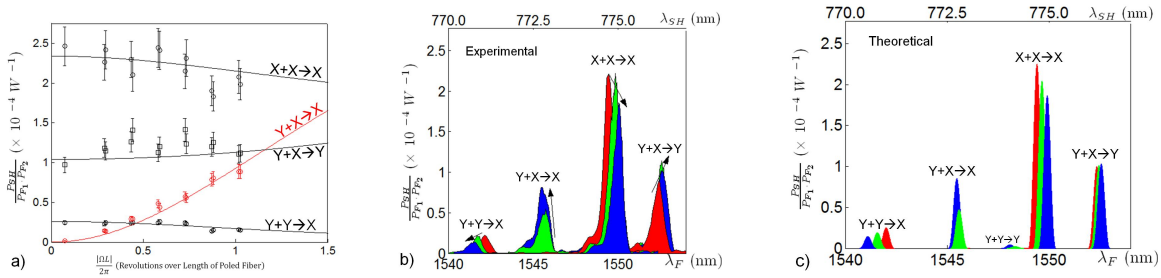

Fig. 2. a) The experimental nonlinear transmittances of the SHG signals plotted against the fiber twist. b) The experimental SHG spectrum for the twisted fiber at varying twists (red = 0 turns, green = 0.66 turns, blue = 0.95 turns). The arrows denote the direction in which the peaks will drift for increasing twist. c) The theoretical SHG spectrum, also at the same three values of the twists as Fig. 2b.

4. Conclusion

We have demonstrated that additional SHG signals in birefringent poled fiber can be generated and their strengths controlled by twisting the fiber. This results from the eigenmodes of the twisted fiber evolving from linearly-polarized to elliptically-polarized, which allows for the intermix of the various $\chi^{(2)}$ tensor elements of the fiber.

We believe that analogous results can be achieved for parametric processes involving the Kerr ($\chi^{(3)}$) nonlinearity by twisting birefringent step-index and microstructured fibers.

References

1. M. Monerie and L. Jeunhomme, Optical and Quantum Electronics **12**, 449–461 (1980).
2. S. Feldman, D. Weinberger, and H. Winful, JOSA B **10**, 1191–1201 (1993).
3. A. Canagasabey, C. Corbari, Z. Zhang, P. G. Kazansky, and M. Ibsen, Opt. Lett. **32**, 1863–1865 (2007).
4. C. Corbari, A. Canagasabey, M. Ibsen, F. Mezzapesa, C. Codemard, J. Nilsson, and P. Kazansky, "All-fibre frequency conversion in long periodically poled silica fibres," in "Optical Fiber Communication Conference, 2005. Technical Digest. OFC/NFOEC," , vol. 5 (2005).